LABORATORI NAZIONALI DI FRASCATI
SIS – Pubblicazioni

LNF–95/064 (P)
11 Dicembre 1995

Sensitivity Limits of a Capacitive Transducer for Gravitational Wave Resonant Antennas

M. Bassan and G. Pizzella
Dipartimento di Fisica, Università Tor Vergata-00133 Roma (Italy)
Istituto Nazionale di Fisica Nucleare, Frascati

ABSTRACT

We analyze the performance of a resonant gravitational wave antenna equipped with a resonant, d.c. biased capacitive transducer, an untuned superconducting matching circuit and a d.c. Squid. We derive simple relations for the detector energy sensitivity that serve as guidelines for device development and we show that, with reasonable improvements in Squid technology, an effective temperature for burst detection of 2 μK can be achieved.

PACS: 0480.+Z

Submitted to Rev. of Scientific Instrument

1. INTRODUCTION

One of the most difficult experimental problems of the gravitational wave research with resonant antennas is the realization of an electromechanical transducer highly coupled to the antenna and with high mechanical and electrical quality factors Q. Furthermore the electronic amplifier, which is part of the transducer itself, must have very low noise, possibly down to a level such to allow detection of one single quantum of the antenna vibrational energy.

Various attempts to realize such a goal have been made since the early seventies. The piezoelectric ceramics used by Weber are powerful devices to detect small vibrations, but they have the drawback that their mechanical Q is small (of the order of 1000) at all temperatures. An important breakthrough [1] was the resonant transducer. It consists of a small mechanical oscillator with resonance frequency equal to that of the antenna. In this way one has a system of two coupled oscillators (antenna and transducer) and the antenna vibration energy can be entirely transferred as mechanical energy to the transducer. To convert this mechanical energy in an electrical signal one can use an inductive (as in Stanford or LSU [2]), capacitive (as in Rome [3]) or parametric (as in Perth [4]) pick-up coupling to the low noise amplifier. Several ways to realize these types of transducer have been devised over the years, by selecting the material, the resonator geometry, the specific electrical pick-up, the matching circuitry and the electronic amplifier. Last, but not least of the technical problems, is then to fasten the transducer to the antenna without degrading its performances.

The purpose of this paper is to show that by using a capacitive resonant transducer coupled to a dc SQUID amplifier via a non resonant matching circuit, one can indeed approach the Giffard limit for sensitivity [5] and, with the expected improvements in dc SQUID technology, the Standard Quantum Limit. We think it is advantageous for the Rome group to push this technology to its limits, and we evaluate what these limits represent in terms of antenna sensitivity to g.w. bursts. The experimental effort required is challenging, and the sensitivity goal, in the 10^{-5} K range, is ambitious for the next five to ten years.

2. RESONATOR GEOMETRY

Mechanical resonators suitable for resonant transducers can be divided into two broad categories: distributed oscillators, like diaphragms [2], mushrooms [3] or flaps [4], and lumped element oscillators, like loaded diaphragms and loaded cantilevers [6]. In the latter class resonating mass and elastic constant are localized in different parts of the resonator, and can therefore be adjusted independently, leaving a greater design freedom. On the other hand, diaphragms and mushrooms must satisfy constraints that relate geometrical and physical quantities, leaving two free parameters among the four quantities R, t, f_y and m_y (radius, thickness, resonant frequency and mass of the resonator)

The results in this paper are derived for a particular geometry (the rosette resonator) recently adopted in some devices of the Rome group [7], but they apply to both classes of resonators except where explicitly stated.

A rosette resonator, schematically shown in fig. 1, is well schematized by a number N_1 of cantilevers that support a disk of mass m_y from its edge.

Note that the loading mass is actually supported by $2N_1$ arms: however the boundary conditions of cantilevers loaded at their center are more appropriate to represent our oscillator, and yield more accurate results, than twice as many cantilevers loaded at the free edge.

For a disk of radius R and thickness h, supported by N_1 pairs of arms of total length L, thickness t and width w, the resonant frequency is given by:

$$f_y = \frac{1}{2\pi}\sqrt{\frac{16N_1Ywt^3}{L^3m_y}} = \frac{2}{\pi^{3/2}}\frac{v_s}{R}\sqrt{\frac{N_1wt^3}{hL^3}} \tag{2.1}$$

where the second expression is derived under the assumption that the central mass and the cantilevers are made of the same material, with Young modulus Y and sound velocity v_S. Eq. (2.1) actually apply to any resonator described by the loaded cantilever model.

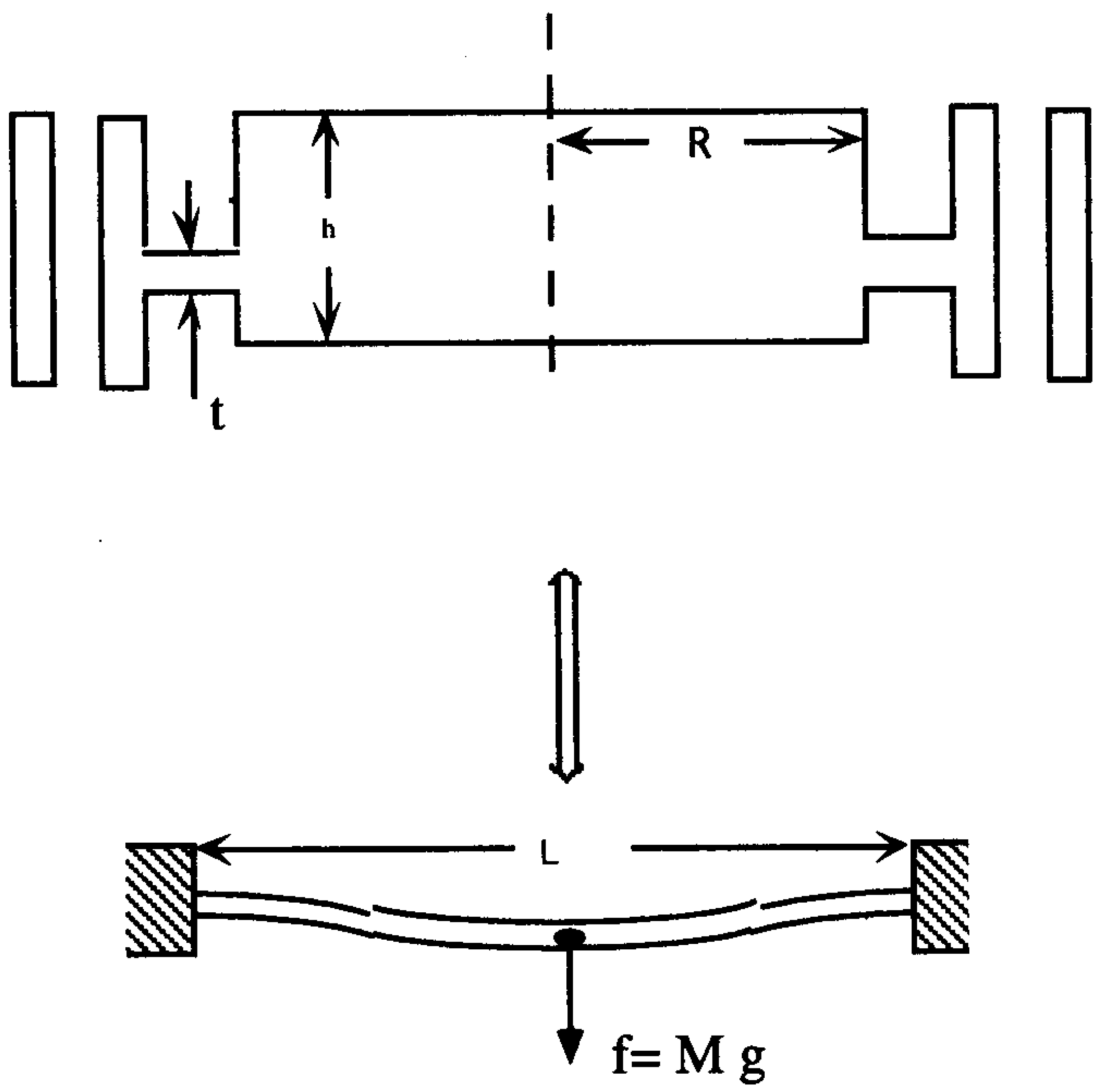

Figure 1 – A loaded cantilever resonator and its conceptual model.

In the case of a rosette resonator, where the arms are curved in order to maximize their length in the available radial space, exact determination of the arm length L is somewhat arbitrary, although effective rules of thumb have been devised.

We can compare Eq. (2.1) with the corresponding relation for distributed resonators:

$$f_y = Av_s\frac{h}{R^2} \tag{2.2}$$

with A =0.49 for a diaphragm or A=0.21 for a mushroom (the Poisson ratio has been taken equal to 0.3).

Clearly Eq. (2.1) depends on more parameters and allows us to independently choose the resonant mass m_y and frequency f_y. However, practical considerations, that will not be discussed here, set a lower limit on the mass m_y : for Alluminium, we get m_y >250 g.

Note that, according to the loaded cantilever model, the central disk moves as a whole, i.e. there is no mode weighting of the amplitude of vibration: in the notation of [3b], $\gamma_t = 1$. This implies that no tuning effect (change of resonant frequency with applied electric field) should arise from the mode shape. In what follows, different resonators with $\gamma_t \neq 1$can be accounted for by multiplying the stored electric field E by γ_t .

3. THE READ OUT CIRCUIT

A capacitive transducer is coupled to a SQUID amplifier via a superconducting matching circuit [8] as shown in fig. 2. The transduction effect is represented by the equivalent voltage generator:

$$v_g = E\,(y\text{-}x) \tag{3.1}$$

where $E = V_b/d$ is the electric field stored in the transducer gap d and y-x is the relative displacement between the transducer (y) and the antenna end face (x). We shall neglect dissipation in the readout circuit: losses are indeed negligible in a superconducting circuit, as long as we keep away from the electrical resonance of the LC circuit of figura 2.

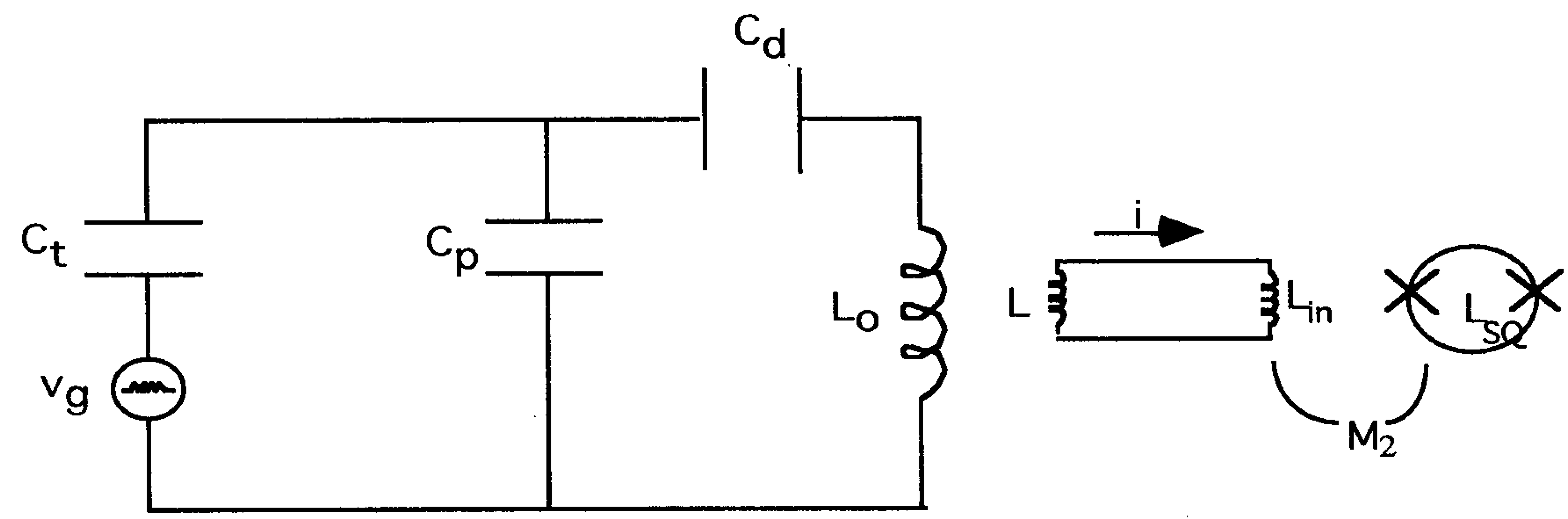

Figure 2 – The read out circuit of the Explorer and Nautilus Antennas. C_t, C_p and C_d are respectively the transducer, stray and decoupling capacitances; L_o and L are the primary and secondary inductances of the super–conducting transformer; L_{in} and L_{SQ} are the input and SQUID loop inductances.

Using Thevenin's theorem the above circuit can be simplified to the following:

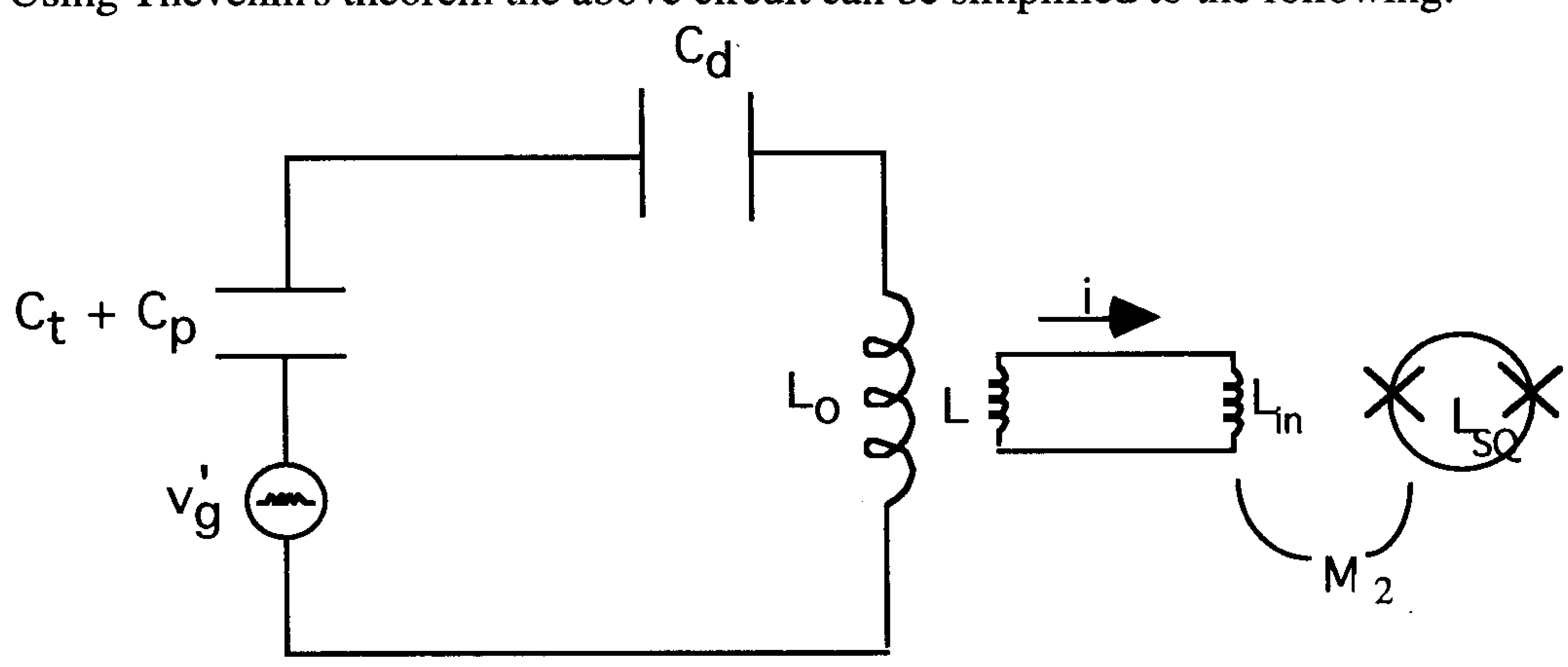

Figure 3 - Equivalent electrical circuit.

where
$$v_g = v_g \frac{C_t}{C_t + C_p} \tag{3.2}$$

Although the scheme of fig. 3 is inaccurate in describing back-action effects (not all the noise current flows into the transducer), it only overestimates its effects by a factor $(C_t+C_p)/C_t$, carrying negligible consequences on our analysis since $C_t >> C_p$.

We define:

$M_1 \equiv k_1 \sqrt{L_0 L}$ the mutual inductance of the matching transformer,

$M_2 \equiv k_2 \sqrt{L_{in} L_{SQ}}$ the mutual inductance between the Squid and its input inductance and

$$\gamma_s \equiv \frac{L}{L + L_{in}}$$

Solving the circuit of fig. 3, neglecting the influence of the SQUID, yields for the current in the secondary coil:

$$i = v_g \frac{C_t}{C_t + C_p} \frac{\sqrt{\frac{L_o}{L}}}{j\omega L_o k_1 - \frac{L + L_{in}}{L} \frac{1}{k_1}\left(\frac{1}{j\omega C} + j\omega L_o\right)} \tag{3.3}$$

where
$$C \equiv \frac{C_d\left(C_t + C_p\right)}{C_d + C_t + C_p} \approx \left(C_t + C_p\right) \tag{3.4}$$

is the combined capacitance as seen from the L_o terminals, and the second equality holds in the usual case $C_d >> C_t + C_p$.

By defining also the transformer effective current gain factor

$$N_e = \sqrt{\frac{L_o}{L}}\, k_1 \frac{L}{L + L_{in}} \tag{3.5}$$

we find
$$i = v_g \frac{C_t}{C_t + C_p} \frac{N_e}{Z_0(\omega)} \tag{3.6}$$

where the resulting impedance is

$$Z_o(\omega) = \frac{1}{j\omega C} + j\omega L_o\left(1 - \gamma_s k_1^2\right) = \frac{1}{j\omega C}\left(1 - \frac{\omega^2}{\omega_{el}^2}\right) \tag{3.7}$$

and the electrical resonance is given by

$$\omega_{el}^2 = \frac{1}{CL_0\left(1 - k_1^2\gamma_s\right)} \tag{3.8}$$

We can now relate the magnetic flux in the SQUID, $\Phi = M_2\, i$, to the mechanical signal

$$\Phi = M_2 i \equiv \alpha_s (y - x) \quad [\mathrm{Wb}] \tag{3.9}$$

with

$$\alpha_s \equiv \frac{C_t}{C_t + C_p} \frac{N_e M_2}{Z_0(\omega)} E \; = j\omega_t C_t \frac{N_e M_2}{\left(1 - \frac{\omega_t^2}{\omega_{el}^2}\right)} E \quad [\mathrm{Wb/m}] \tag{3.10}$$

where eq. (3.4) and (3.7) have been used. We find that in Eq. (3.10) the factors (C_t+C_p) cancel out, except for a weak dependence in ω_{el}. We can then draw the unexpected conclusion that, as long as the electrical frequency is well above the operating frequency $f_y = \omega_y / 2\pi$, the transduction coefficient α_s is unaffected by the stray capacitance C_p.

Eq. (3.10) holds for any capacitive transducer equipped with the circuit of fig. 2. For a mushroom or diaphragm resonator, due to eq. (2.2) linking resonant frequency and geometry, one finds that the product $\omega_t C_t$ simplifies to a constant times t/d [9]. This is not the case for the other resonators considered here.

Note that, in order to maximize the signal fed to the SQUID (as long as the electrical frequency is maintained above the antenna resonance), we find the obvious prescription to make a transducer with the largest active capacitance, and a transformer with large coupling coefficient and turn ratio (but keeping the secondary coil L close to the SQUID input coil L_{in}. The SQUID mutual inductance M_2 is usually not at the experimenter's disposal, and the electric fields E is turned up as high as it is safe and practical ($E < 2\; 10^7$ V/m).

4. THE SIGNAL - SYSTEM RESPONSE TO AN IMPULSIVE EXCITATION

Consider an impulsive (delta-like) force acting on the antenna:

$$F_x(t) = F_o\, \delta(t) \quad [\mathrm{N}] \tag{4.1}$$

The amplitude of vibration of the end face of the bar turns out to be:

$$x = \frac{F_o}{m_x} \frac{1}{\omega_+^2 - \omega_-^2} \left(\frac{\omega_+^2 - \omega_y^2}{\omega_+} \sin\omega_+ t - \frac{\omega_-^2 - \omega_y^2}{\omega_-} \sin\omega_- t \right) \tag{4.2}$$

where the eigenfrequencies of the two normal modes for the coupled antenna-transducer system are:

$$\omega_\pm^2 = \frac{1}{2}\left[\omega_y^2(1+\mu) + \omega_x^2 \pm \sqrt{\left(\omega_y^2(1+\mu) + \omega_x^2\right)^2 - 4\omega_x^2\omega_y^2} \right] \tag{4.3}$$

where $\mu \equiv m_y / m_x$ is the ratio of the equivalent masses of transducer and antenna and is, for any realistic system, $\mu \ll 1$.

The response of the transducer is given by

$$y - x = \frac{F_o}{m_x} \frac{1}{\omega_+^2 - \omega_-^2} [-\omega_+ \sin(\omega_+ t) + -\omega_- \sin(\omega_- t)]$$

or, separately considering each normal mode:

$$(y - x)_\pm = \frac{F_o}{m_x} \frac{1}{\omega_+^2 - \omega_-^2} \omega_\pm \sin(\omega_\pm t) \tag{4.4}$$

Eq. (4.4) shows that both modes respond with virtually the same amplitude of vibration to an impulsive force, regardless of the degree of tuning of the transducer. A well tuned transducer ($\omega_y = \omega_x$) has the advantage of a much larger response for both modes, because the denominator in Eq. (4.4) assumes its minimum value.

Indeed, in the well tuned case and with $\mu \ll 1$, we get

$$\omega_\pm^2 = \frac{1}{2}\left[\omega_x^2 \pm \sqrt{\mu}\right] \tag{4.5}$$

so that:

$$(y - x)_\pm = \frac{F_o}{2\,\omega_x^2\, m_y} \omega_\pm \sin\,(\omega_\pm t) \tag{4.6}$$

5. DISSIPATION AND BROWNIAN NOISE

The losses of the antenna and transducer are characterized by amplitude decay times τ_x and τ_y. These in turn determine those of the two normal modes $\tau_\pm$.

At each mode the thermal noise variance is given by:

$$\overline{(y - x)^2_{\pm Br.}} = \left\{ \left|W_{yx}(\omega_\pm)\right|^2 \frac{4k_B T m_x}{\tau_x} + \left|W_{yy}(\omega_\pm)\right|^2 \frac{4k_B T m_y}{\tau_y} \right\} \tau_\pm^{-1} \tag{5.1}$$

where T is the thermodynamic temperature and k_B the Boltzmann's constant. The transfer functions are:

$$W_{yx} = \frac{\omega^2}{m_x D(\omega)}$$

$$W_{yy} = \frac{-\omega^2 + \omega_x^2 + 2j\omega/\tau_x}{m_y D(\omega)} \tag{5.2}$$

$$D(\omega) = [-\omega^2 + \omega_x^2 + \mu\omega_y^2 + j\omega(2/\tau_x + 2\mu/\tau_y)][-\omega^2 + \omega_y^2 + 2j\omega/\tau_y] -$$

$$-[\mu\omega_y^2 + 2j\omega\,\mu/\tau_y][\omega_y^2 + 2j\omega/\tau_y]$$

In the optimal case of a well tuned transducer we compute, using Eq. (3.9) the magnetic flux coupled into the SQUID by the Brownian noise:

$$(\Phi_+)_{Br.} \approx (\Phi_-)_{Br.} = \alpha_s \sqrt{\frac{k_B T}{2 m_y \omega_\pm^2}} \tag{5.3}$$

We remark that this calculation holds only as long as the resonant interaction of the electrical resonator LC with the mechanical resonators can be neglected. Otherwise, a different analysis considering three normal modes on equal footing must be applied. Besides, the noise spectra of the two normal modes must not overlap, so that we can analyze them separately: this is true as long as the mode separation is larger than their intrinsic bandwidth (see below, sect.8):

$$\Delta\omega = \omega_x \sqrt{\mu} \geq 4\beta_3. \tag{5.4}$$

6. THE COUPLING COEFFICIENT β

The transducer energy coupling coefficient β is, in many respects, the figure of merit of a transducer. It is defined as the fraction of mechanical energy that the transducer is capable of converting in electrical energy during one period of oscillation.

It is convenient to define β at the SQUID input, where the noise sources are referred:

$$\beta = \frac{\frac{1}{2} L_{in} \overline{i^2}}{\frac{1}{2} \frac{F_o^2}{m_x}} \tag{6.1}$$

where an impulsive excitation (Eq. (4.1)) has been considered and the magnetic energy is evaluated at the SQUID input coil L_{in}.

With the aid of Eq. (3.6) and (4.4) we find:

$$\beta = \frac{L_{in}}{2m_x} \left(\frac{C_t}{C_t + C_p} \right) \left(\frac{N_e E}{|Z_o|} \right)^2 \frac{\omega_+^2 + \omega_-^2}{\left(\omega_+^2 - \omega_-^2\right)^2} \tag{6.2}$$

that can be re-expressed, using Eq. (3.8), as

$$\beta = \frac{\alpha_s^2}{2 m_x L_{SQ}} \frac{\omega_+^2 + \omega_-^2}{\left(\omega_+^2 - \omega_-^2\right)^2} = \frac{\alpha_s^2 L_{in}}{2 m_x M_2^2} \frac{\omega_+^2 + \omega_-^2}{\left(\omega_+^2 - \omega_-^2\right)^2} \tag{6.3}$$

These equations hold in the general case. They can be simplified for a well tuned transducer to

$$\beta = \frac{L_{in}}{4\omega_x^2 m_t} \left(\frac{\alpha_s}{M_2} \right)^2 \tag{6.4}$$

7. THE AMPLIFIER NOISES AND THE BACK ACTION.

The SQUID amplifier [10] contributes both a wide band flux noise in the SQUID, with spectral density ϕ_n, that we express in unit of $\frac{\Phi_o}{\sqrt{Hz}}$ (Φ_o = 2.07 10^{-15} Wb is the flux quantum) and a current noise circulating in the SQUID. These two noise sources can be represented by a current noise and a voltage noise generators at the SQUID input. The voltage noise is responsible for the back action effect. The voltage noise V_n in practical d.c. SQUID amplifiers has not yet been measured (or even detected), but reasonable estimates [9] predict $V_n \approx 1.5\ 10^{-16}$ V/√Hz at 1 kHz.

In the devices presently used in the Rome group [8] the measured wide band flux noise $\phi_n = 2\ 10^{-6}\Phi_o/\sqrt{Hz}$ corresponds to a current noise $I_n = \phi_n/M_2 = (2\ 10^{-6}\ \Phi_o/\sqrt{Hz}/2\ 10^{-9}\ H) = 2\ 10^{-12}$ A/√Hz. From this we can estimate the amplifier noise temperature $T_n = V_n I_n / k_B \approx 20\ \mu K$.

7.1 The noise match impedance ratio λ

The parameter λ is defined as the ratio between the optimum noise match impedance of the amplifier and its actual input impedance. For the SQUID of fig. 2 it takes the value:

$$\lambda = \frac{I_n}{V_n} \cdot \omega \left(L_{in} + L \left(1 - k_1^2 \frac{\omega^2}{\omega_{el}^2 - \omega^2} \right) \right) \tag{7.1}$$

For a SQUID with the above noise sources we find λ≈1 00.

7.2 Back Action

The back action is a noise force exciting the modes due to the SQUID voltage noise, with a transfer function almost identical to that of the transducer Brownian noise. It is, in all respects, indistinguishable from the thermal noise, so that it can be described by an increase in the thermodynamic temperature of each mode [11]:

$$T_{e=} = T + T_{b.a.} = T + \frac{\beta Q T_n}{2\lambda} \tag{7.2}$$

It depends on the voltage noise (T_n/λ) and it is therefore not observed in the present detectors equipped with d.c. SQUIDS. Anyway, with the above estimates for the SQUID voltage noise, we conclude that the back action can be neglected with respect to a bath temperature T=100 mK, as long as $\beta Q < 10^5$.

8. ANTENNA SENSITIVITY FOR G.W. BURSTS (TUNED TRANSDUCER)

From now on we shall assume the resonant transducer to be perfectly tuned to the antenna for optimal response. The sensitivity of the antenna to a short burst of gravitational radiation is expressed by means of the effective temperature, that can be computed, as long as condition (5.4) holds, by the relation [12]:

$$T_{eff} = \frac{\Delta E_{min}}{k_B} \approx 4\, T_e \sqrt{\Gamma} \tag{8.1}$$

where T_e is the bath temperature including back action (Eq. 7.2) and Γ is the ratio between wide band and resonant noise:

$$\Gamma = \frac{\phi_n^2}{2\,\tau\,\Phi_{Br}^2} = \frac{T_n}{2\,T_e\,\beta\,Q}\left(\lambda + \frac{1}{\lambda}\right) \qquad (8.2)$$

We shall assume, in what follows, that back action adds a negligible noise, and therefore we ignore it. From Eq. (8.1), (8.2) and (5.3) we find

$$k_B T_{eff} = \frac{4\phi_n\omega}{\alpha_s}\sqrt{\frac{m_y k_B T}{\tau}} \qquad (8.3)$$

It is interesting to note that (8.3) is valid in general for any linear transducer, as $\phi_n\,\omega/\alpha_s$ is just the equivalent noise velocity at the antenna input and the second term is the equivalent brownian force [5].

Substituting Eq. (3.11) for α_s we get

$$k_B T_{eff} = \frac{4\phi_n}{N_e M_2 C_t}\left(1 - \frac{\omega^2}{\omega_e^2}\right)\frac{1}{E}\sqrt{\frac{k_B T}{\tau}m_y} \qquad (8.4)$$

showing that, as far as the transducer geometry is concerned, one should minimize the ratio $\frac{\sqrt{m_y}}{C_t}$: a small mass transducer is desirable, whitin the limits discussed in next section, but with a large capacitance: hence the importance of achieving a small gap. Assuming that the resonator has a simple disk geometry, so that $C_t = \varepsilon_0\pi\,R^2/d$ and $m_y = \rho\pi\,R^2\,h$ (as for all transducers considered in sect.2, but the flap) we can write:

$$T_{eff} = \left[\frac{4}{\varepsilon_0\sqrt{\pi k_B}}\right]\cdot\left[\frac{1}{N_e}\left|1 - \frac{\omega^2}{\omega_e^2}\right|\right]\cdot\left[\frac{\sqrt{h\rho}}{R}\frac{d}{E}\right]\cdot\left[\frac{\phi_n}{M_2}\right]\cdot\sqrt{\frac{T}{\tau}} \qquad (8.5)$$

where we grouped five terms:

-the first is a universal constant, equal to 6.86 10^{22} I.S. units,

-the second depends on the electric properties of the superconductive transformer,

-the third depends on the transducer mechanical parameters and stored field,

-the fourth on SQUID coupling and noise

-and the last one on the mode temperature and decay time.

Note that for mushrooms and diaphragms the ratio $\frac{\sqrt{h}}{R}$ is set by the resonant frequency, as shown by eq.(2.2), so that T_{eff} has no dependence on the resonator shape and size, except for the gap[9].

9. OPTIMUM MASS, BANDWIDTH AND III MATCHING CONDITION

The antenna (or, rather, the mode) bandwidth (FWHM) is the characteristic frequency of the Wiener filter, and is the inverse of the optimum sampling time[11]:

$$\Delta\omega = 2\beta_3 = \frac{2}{\tau\sqrt{\Gamma}} \approx \frac{8T}{\tau T_{eff}} \quad \text{[rad/s]} \tag{9.1}$$

$$\beta_3 = \frac{\alpha_s}{\phi_n \omega}\sqrt{\frac{k_B T}{m_y \tau}}$$

where Eq. (8.1) and (8.3)have been used.

We have mentioned earlier that the transducer mass cannot be made small at will, even if this apparently yields a large bandwidth and a low T_{eff}. Indeed the III matching condition, derived in ref.[11] for the particular case of vanishing thermal noise, can be cast in a more general form as:

$$\mu \geq \frac{4\beta}{1+\lambda^2}\left(\frac{2T\lambda}{T_n Q} + \beta\right) \tag{9.2}$$

where the second term, representing the back action, is usually much smaller than the first, thermal one. This relation can be derived in several different ways and states, as already pointed out in (5.4), that the SNR frequency curves of the two normal modes should not overlap.

When the dependence on the transducer mass m_y in μ and β is worked out, one finds [13] (as long as λ>>1 and neglecting back action)

$$m_y = 4\frac{\alpha_s}{\omega_x^2 \phi_n}\sqrt{\frac{k_B T m_x}{\tau}} \tag{9.3}$$

We want to stress that all equations derived in sects. 5 through 9 hold for detectors equipped with capacitive transducers with a resonating mass larger than or equal to this value. For lighter transducers a different approach must be taken [14], as the single mode analysis breaks down.

Moreover, Eq. (9.3) neglects back action, and is inaccurate when its effects are significant. As T_{ba} depends on m_y (Eq. 7.2 and 6.5), a more elaborate optimization is required, yielding a larger value for m_y.

When the transducer mass is optimized according to (9.3), we find the detection noise temperature

$$k_B T_{eff} = 8\left[\frac{\phi_n}{\alpha_s}\right]^{1/2} m_x^{1/4}\left[\frac{k_B T}{\tau}\right]^{3/4} \tag{9.4}$$

showing that the detector sensitivity to g.w. burst flux $F(\omega) = k_B T_{eff} / \Sigma$ (where Σ is the cross section, proportional to m_x) improves slightly less than linearly with the antenna mass.

We have not addressed the issue of tuning the LC circuit to the mechanical modes. This tuned configuration was tested in one of the Nautilus preliminary runs, and several practical disadvantages have emerged that have convinced us to procrastinate the adoption of this solution: mainly, one has to deal with three modes, experimentally a more complex and critical system, without achieving sufficient benefit [14,15].

10. NUMERICAL EXAMPLES AND CONCLUSION

We remark that the above considerations have been fully tested experimentally with the antennas of the Rome group [8] to the level of $T_{eff} \approx 5$ mK.

We now evaluate T_{eff}, bandwidth and optimum transducer mass and mode spacing (beat frequency) and show the results in Table I.

The first column reports parameter values already attained with a mushroom transducer, and represents the state of the art of our antenna-transducer system: the sensitivity of 280 μK will be reached on the Nautilus ultracyogenic detector [16] when the system tune-up is completed, with elimination of all external noise. Note that in the present set up the transducer is much heavier (300 g) than the optimum value, because the latter is not compatible with the achieved active capacitance of 4 nF. A constrained optimization is possible with numerical methods [14].

In the second column we foresee reasonable improvements, within the reach of present technology. The sensitivity of 19 μK could be achieved in the near future.

The third column reports more optimistic, but by no means unreasonable values: however, at the level of sensitivity here discussed, sounder estimates of the SQUID voltage noise are needed, in order to appropriately account for back action effects.

The small value for ϕ_n implies, besides foreseable SQUID fabrication advances [17], also the development of an improved second stage amplifier. The large capacitance of 20 nF can be achieved either by reducing the gap to values of the order of 6 μm, or by using two electrodes in a push-pull configuration.

We believe that a few resonant antennas with such a sensitivity will be a powerful mean to search for gravitational waves in a still unknown Universe.

Table I - Performance of the Nautilus ultracryogenic g.w. detector equipped with present, advanced and very advanced capacitive transducers.

PARAMETERS	State of the art	Near future	Optimistic
C_t (F)	4.2E-9	1.2E-8	2.0E-8
C_p (F)	6.0E-10	3.0E-10	2.0E-10
d(μm)	49	10	6
L_o (H)	2.9	2.0	2.0
L (H)	8.0E-7	1.0E-6	1.0E-6
L_{in} (H)	1.0E-6	1.0E-6	1.0E-6
k_1	0.77	0.8	0.9
L_{sq} (H)	5.60E-11	5.00E-11	5.00E-11
k_2	0.5	0.6	0.7
M_1 (H)	1.16E-03	1.13E-03	1.27E-03
γ_s	0.44	0.50	0.50
N_e	647	566	636
M_2 (H)	3.7E-9	4.2E-9	4.9E-9
f_{el} (Hz)	1584	1231	1027
T (K)	0.1	0.1	0.1
τ (s)	500	1000	2000
ϕ_n ($\phi_o/\sqrt{(Hz)}$)	2.0E-6	1.0E-6	2.0E-7
Vn (estimate)	1.5E-16	1.5E-16	1.5E-16
Tn (estimate)	1.2E-5	5.1E-6	8.7E-7
E (V/m)	8.0E+6	1.0E+7	1.0E+7
m_y (kg)	0.30	0.28	4.28
PERFORMANCES			
α_s (Wb/m)	6.8E-4	3.5E-3	1.5E-2
β	8.6E-4	1.9E-2	1.8E-2
M_{y}_opt	0.038	0.276	4.280
λ	53	24	4
Tba (estimate)	1.3E-4	5.7E-3	1.2E-2
Teff (μK)	280	19	2
Bandwidth at each mode. (Hz)	0.90	7	29
mode spacing (Hz)	15	14	55

ACKNOWLEDGMENTS

We are grateful to C.Cosmelli, G.V.Pallottino, Y.Minenkov and M.Visco for useful discussions and suggestions.

REFERENCES

[1] H.J.Paik, J. Appl. Phys **47,** 1168 (1976).
[2] N.Solomonson, W.O.Hamilton ,W.W. Johnson: Rev.Sci.Instrum. **65**, 174 (1994).
[3] P.Rapagnani, Nuovo Cimento **5C** 385, (1982);
Y Ogawa, P.Rapagnani: Nuovo Cimento **7C**, 21, (1984) .
[4] M.E.Tobar, D.G.Blair: J.Phys.D: Appl.Phys. **26** , 2276 (1993).
[5] R.P.Giffard: Phys.Rev.D, **14**, 2478 (1976)
[6] R.J.Roark *Formulas for stress and strain* Mc Graw Hill, New York and London, 1943
[7] M.Bassan, Y.Minenkov, G.Zaccarian: "*Resonators of novel geometry for large mass resonant transducers*" Proc. of the first Edoardo Amaldi Conference on Gravitational Wave Experiments, Frascati 1994, Word Scientific 1995.
[8] P.Astone, M.Bassan, P.Bonifazi, P.Carelli, M.G.Castellano, G.Cavallari, E.Coccia, C.Cosmelli, V.Fafone, S.Frasca, E.Majorana, I.Modena, G.V.Pallottino, G.Pizzella, P.Rapagnani, F.Ricci, M.Visco: Phys Rev D47, 362.
[9] C.Cosmelli: Europhys. Lett. **16,** 17 (1991).
[10] R. Leoni, G. Schirripa Spagnolo, P. Carelli and M. Pullano
J. Appl. Phys. 68, 4304-4309 (1990).
[11] G.V.Pallottino, G.Pizzella: Il Nuovo Cimento **4C**, 237, (1981)
[12] G.Pizzella: Il Nuovo Cimento **2C**, 209, (1979).
[13] M.Bassan: Class. Quantum Grav. 11, A39 (1994) .
[14] S.Turolla- Thesis Universita' Tor Vergata (unpublished)
M.Bassan-S.Turolla: in preparation.
[15] C.Cosmelli Europhys Lett. **16C**,319 (1993)
[16] P.Astone, M.Bassan, P.Bonifazi, F.Bronzini, M.G.Castellano, E.Coccia, C.Cosmelli, V.Fafone, S.Frasca, E.Majorana, I.Modena, G.V.Pallottino, G.Pizzella, P.Rapagnani, F.Ricci, M.Visco: Europhysics Letters 16,231-235, (1991).
[17] P.Carelli, private communication (1995).